A new look at an old concept: Using $^{15}N_2O$ isotopomers to understand the relationship between soil moisture and N_2O production pathways

Kate A. Congreves[1], Trang Phan[1], and Richard E. Farrell[2]

[1]Department of Plant Sciences, [2]Department of Soil Science, University of Saskatchewan, Saskatoon, SK S7N 5A8

Correspondence to: Kate A. Congreves (kate.congreves@usask.ca)

Abstract

Understanding the production pathways of potent greenhouse gases, such as nitrous oxide (N_2O), is essential for accurate flux prediction and for developing effective adaptation and mitigation strategies in response to climate change. Yet, there remain surprising gaps in our understanding and precise quantification of the underlying production pathways – such as the relationship between soil moisture and N_2O production pathways. A powerful, but arguably underutilized, approach for quantifying the relative contribution of nitrification and denitrification to N_2O production involves determining $^{15}N_2O$ isotopomers and ^{15}N site preference (SP) via spectroscopic techniques. Using one such technique, we conducted a short-term incubation where N_2O production and $^{15}N_2O$ isotopomers were measured 24-h after soil moisture treatments of 40 to 105% water-filled pore space (WFPS) were established – for each of three soils that differed in nutrient levels, organic matter and texture. Relatively low N_2O fluxes and high SP values indicted nitrification during dry soil conditions, whereas at higher soil moisture, peak N_2O emissions coincided with a sharp decline in SP indicating denitrification. This pattern supports the classic N_2O production curves from nitrification and denitrification as inferred by earlier research; however, our isotopomer data enabled the quantification of source partitioning for either pathway. At soil moisture levels < 53% WFPS, the fraction of N_2O attributed to nitrification (F_N) predominated but thereafter decreased rapidly with increasing soil moisture (x), according to: $F_N = 3.19 - 0.041x$, until a WFPS of 78% was reached. Simultaneously, from WFPS of 53 to 78%, the fraction of N_2O that was attributed to denitrification (F_D) was modelled as: $F_D = -2.19 + 0.041x$; at moisture levels of > 78%, denitrification completely dominated. Clearly, the soil moisture level during transition is a key regulator of N_2O production pathways. The presented equations may be helpful for other researchers to estimate N_2O source partitioning when soil moisture falls within the transition from nitrification to denitrification.

1. Introduction

Soils are the largest source of anthropogenic N_2O emissions, accounting for up to 80% of total N_2O emissions (Environment Canada, 2015). Understanding the mechanisms leading to the emission of this potent greenhouse gas is essential for accurate flux prediction and for developing effective adaptation and mitigation strategies in response to climate change. Decades of research have strengthened our understanding of N_2O fluxes—namely, how N_2O production is regulated by soil oxygen, substrate availability, and microbial activity (Butterbach-Bahl et al., 2013; Chapuis-Lardy et al., 2007; Wagner-Riddle et al., 2017); as well as how N_2O emission is regulated by advection,

solubility and diffusion (Balaine et al., 2013; Clough et al., 2005). Indeed, our understanding of the relationship between N_2O production and soil moisture has benefited greatly from the use of ^{15}N tracers (Bateman and Baggs, 2005; Stevens and Laughlin, 1997; Groffman et al., 2006). However, there remain surprising grey-areas in our understanding of the underlying mechanisms, one such area being the precise relationship between soil moisture and

5   N_2O production pathways, especially during the transition from one dominant pathway to another (Bateman and Baggs, 2005).

Nitrous oxide is a product of nitrification and denitrification—microbially driven processes that depend on the aeration status of the soil (Banerjee et al., 2016; Barnard et al., 2005). As a result, the relative contributions of nitrification and denitrification are often determined based on their relationship to soil water-filled-pore space (WFPS), which acts as

10   a proxy for aeration status. However, the widely cited relationship between soil N_2O production and soil moisture (Fig. 1) is actually an educated deduction that blends work from two different studies, from which the N_2O production pathways are inferred (Davidson, 1991; Linn and Doran, 1984). As such, it may be argued that the precise relationship between soil water content and N_2O production mechanisms remains unclear and requires more complete quantification. While previous research has provided important steps towards better quantifying the relationship using

15   ^{15}N enrichment and acetylene inhibition techniques (Bateman and Baggs, 2005), natural abundance ^{15}N techniques may provide superior information by imposing fewer confounding effects on step-wise N transformations.
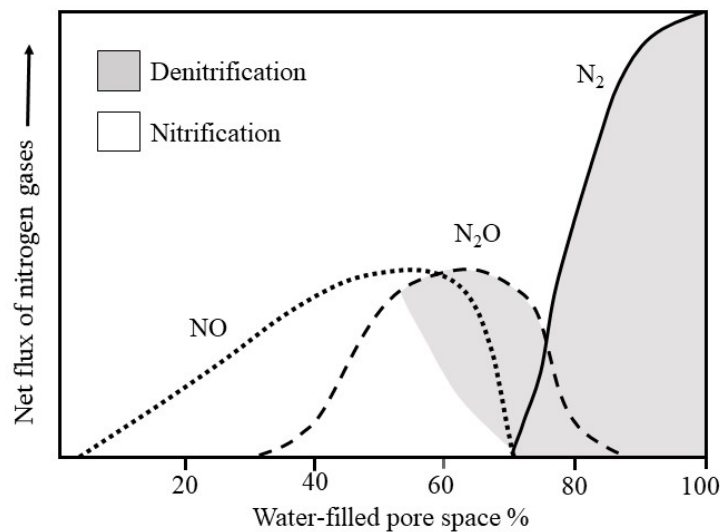
Figure 1 Relative contributions of nitrification and denitrification processes to N_2O production as a function of water-filled pore space (adapted from Davidson 1991).

20   Isotopomers—i.e., isomers having the same number of each isotopic atom, but differing in their position (McNaught and Wilkinson, 1997; Ostrom and Ostrom, 2012)—provide a powerful and novel approach for quantifying the relative contribution of N_2O producing processes via nitrification and denitrification (Van Groenigen et al., 2015). Early work focused on the intramolecular distribution of ^{15}N within the linear N_2O molecule (Sutka et al., 2006; Toyoda et al.,

2005), investigations of atmospheric or oceanic N_2O isotopomers (Popp et al., 2002; Toyoda and Yoshida, 1999; Yoshida and Toyoda, 2000), and soil emitted N_2O isotopomers (Perez et al., 2001; Yamulki et al., 2001). The isotopomers of N_2O (i.e., $^{14}N^{15}NO$ and $^{15}N^{14}NO$) can be quantified using advanced laser spectroscopic approaches—including cavity ring-down spectroscopy (CRDS)—that enable the intramolecular ^{15}N distribution of N_2O to be determined (Mohn et al., 2014). The difference between the abundance of ^{15}N within the central (alpha, α) and the terminal (beta, β) N atoms of the linear N_2O molecule is expressed as site-preference (SP), and high SP values of 13 to 37‰ are attributed to nitrification (hydroxylamine oxidation) while SP values of 0‰ or less indicate nitrite or nitrate reduction (denitrification and nitrifier denitrification) (Denk et al., 2017; Ostrom et al., 2010; Sutka et al., 2006; Toyoda et al., 2005). The underlying reason for the distinct differences in SP values of N_2O from either microbial pathway is due to primary kinetic isotope effects when N_2O is produced (Popp et al., 2002).

Our objective was to use $^{15}N_2O$ isotopomers to precisely quantify the relationship between soil moisture and N_2O production in soils differing in soil nutrient level, organic matter, and texture.

2. Materials and Methods

2.1 Soil collection and characterization

Surface (0–10 cm) soils representing different nutrient levels and texture classes were collected from three locations in the Dark Brown soil zone in Saskatchewan, Canada. The soils—classified as Dark Brown Chernozems of the Sutherland, Asquith and Bradwell associations—were collected using a shovel, air dried and sub-samples were shipped to A&L Laboratories Inc (London, ON) for analysis (Table 1). For additional characterization, sub-samples were analyzed at the University of Saskatchewan for equilibrium soil water content, soil inorganic N levels, soil total N concentration and ^{15}N abundance (Table 1). The equilibrium soil water was determined via the long-column method based on the average of four technical replicates (Reynolds and Topp, 2007). Initial soil NO_3^- and NH_4^+ concentrations were determined in quadruplicate using the KCl extraction method of Maynard et al. (2007); briefly, 5 g soil was mixed with 50 mL of 2 M KCl, shaken for 30-min, filtered through Whatman 42 filter paper, and the extracts frozen at -20°C until they could be analyzed. For analysis, the extracts were thawed and allowed to equilibrate to room temperature before being analyzed using air segmented (continuous) flow analysis with a SEAL AA3 HR chemistry analyzer (SEAL Analytical; Kitchener, ON). Soil total N concentration (%) and ^{15}N content (atom%) were determined in duplicate using a Costech ECS4010 elemental analyzer (Costech Analytical Technologies Inc., Valencia CA) coupled to a high-precision Delta V mass spectrometer (Bremen, Germany) with a precision of 0.06‰ for $\delta^{15}N$. Chickpea flour with an atom% $^{15}N = 0.3691$ was used as a lab reference.

2.2 Incubation experimental design

For the incubation study, soil microcosms were established over a range of moisture treatments for each soil, and arranged in a completely randomized design with four replicates. For each microcosm, sieved (2-mm mesh screen) and air-dried soil was packed into a small (5.9 cm i.d. × 0.80 cm tall) plastic petri dish. The mass of soil needed to fill the petri dish varied with texture—ranging from 22.0 g to 29.0 g—and yielded soil bulk densities of 1.01, 1.10, and

1.33 g cm^{-3} for the Sutherland, Asquith, and Bradwell soils, respectively. While the quantities and bulk densities differed for each soil type, it was essential that the soil completely fill the petri dishes to avoid any differences in soil surface boundary layer or gas diffusion that would alter N$_2$O emission.

Soil moisture treatments were based on gravimetric soil water content (θg) established by adding deionized water to the soil microcosms, using a fine mist of water applied from a manual spray bottle, to a predetermined weight. Gravimetric soil moisture content was varied to yield a water-filled pore space (WFPS) between 40 and 105%.

The gravimetric water, volumetric water, and WFPS were determined according to Eq. (1-3):

$$Gravimetric\ water\ \theta_g(g\ H_2O\ \ g\ soil^{-1}) = \frac{water\ added\ (g)}{dry\ soil\ (g)} \tag{1}$$

$$Volumetric\ water\ \theta_v\ (cm^3 H_2O\ \ cm^3\ soil^{-1}) = \ \theta_g\ \times BD \tag{2}$$

$$\%\ WFPS = \left[\frac{\theta_v}{\left(1-\frac{BD}{PD}\right)}\right] \times\ 100 \tag{3}$$

where, BD denotes soil bulk density and PD denotes particle density (PD), which was assumed to be 2.65 g cm^{-3}.

Immediately after moistening the soil microcosm, the petri dish was sealed inside a 1L wide-mouth mason jar fitted with a gas sampling septum, and time of sealing was recorded. Blank jars containing an empty petri dish were set up to account for background (atmospheric) gas concentrations. The microcosms were incubated at 22°C ± 1°C for 24-h.

2.3 Sampling and analysis

After 24-h, a headspace gas sample was collected from each microcosm (with the time of sampling recorded) using a 20-mL plastic syringe fitted with a 22-gauge needle, injected into an evacuated 12-mL Exetainer® tube (Labco Limited, UK), and analyzed for N$_2$O, CO$_2$, and O$_2$ concentration using gas chromatography (Bruker 450 GC, Bruker Biosciences, Billerica, MA). Immediately thereafter, a separate 30-mL gas sample was collected from each microcosm, injected into an evacuated 12-mL Exetainer® tube, and analyzed for ^{15}N$_2$O concentration, δ^{15}N$_\alpha$, δ^{15}N$_\beta$, and δ^{18}O using a CRDS-based Picarro G5131-i isotopic N$_2$O analyzer (Picarro Inc.; Santa Clara, CA).

2.4 Isotopomer approach using ^{15}N site preference and $\boldsymbol{\delta^{18}}$O for N$_2$O source identification

Site preference was calculated by subtracting the abundance of ^{15}N from the terminal N atom (beta, β) from that of the central (alpha, α) N atom. The fraction of N$_2$O derived from hydroxylamine oxidation during nitrification (F$_N$) or the reduction of nitrate or nitrite during denitrification (F$_D$) was estimated for each soil by adopting the isotopomer mixing approach used by others (Deppe et al., 2017; Lewicka-Szczebak et al., 2017; Zou et al., 2014), and which use

the ^{15}N SP and δ^{18}O values of gas samples collected from the soils. As suggested by Lewicka-Szczebak et al. (2017) and by Well et al. (2012), and because SP was more closely correlated to δ^{18}O (r = 0.906) than δ^{15}N (r = 0.849), we used the relationship between δ^{15}N SP and δ^{18}O, instead of δ^{15}N SP and bulk δ^{15}N. Equations (4) and (5) show the source partitioning calculations.

$$F_N = \frac{SP_x - SP_D}{SP_N - SP_D} \qquad (4)$$

$$F_D = 1 - F_N \qquad (5)$$

10   where F_N and F_D indicate the fraction of N_2O derived from nitrification or denitrification, respectively; SP denotes the site preference for the sample (SP_x) and the endmembers for nitrification (SP_N) and denitrification (SP_D).

Rather than relying on average literature-derived endmembers like previous work (Deppe et al., 2017; Lewicka-Szczebak et al., 2017), we used soil-specific endmembers derived from our data to perform the linear mixed model. This is because we measured a wide range of soil WFPS treatments with high frequency between dry and moist

15   conditions for each soil, enabling us to determine the point at which the δ^{15}N SP or δ^{18}O values either dropped or increased as soil WFPS changed (as precisely as the data permitted) indicating a transition from nitrification to denitrification. This approach is consistent with earlier recommendations that data be collected at high enough frequencies to capture gradual changes in isotope values as influenced by traditional proxies (i.e., gradual changes in soil WFPS) (Decock and Six, 2013a). However, it must be noted that the underlying assumption is that the soil-specific

20   endmembers are more reflective of the transition from nitrification to denitrification in each of the soils tested herein, than general literature-derived endmembers would be for any one soil. Moreover, it is assumed that the endmembers represent N_2O produced when the sole source was either nitrification or denitrification. Endmembers for SP_D to SP_N were set at: 2.0 to 23.7; 0.7 to 21.7; 14.4 to 23.3 for the Sutherland, Asquith, and Bradwell soils, respectively. Endmembers for $\delta^{18}O_D$ to $\delta^{18}O_N$ were set at: 16.0 to 35.1; 18.8 to 39.5; 25.4 to 34.2 for the Sutherland, Asquith, and

25   Bradwell soils, respectively. The endmember ranges were based on our data where $SP_N/\delta^{18}O_N$ represented the average values before the transition zone from nitrification to denitrification-dominated N_2O production; $SP_D/\delta^{18}O_D$ represented the lowest values during denitrification for each soil type. For source partitioning, the influence of N_2O reduction to N_2 on SP was taken into account by using the reduction and mixing line intercept approach – as described by Deppe et al. (2017) and Lewicka-Szczebak et al. (2017). However, rather than using an estimated reduction line

30   derived from the literature, we calculated the slope and intercept for the reduction line based on our data: the SP/δ^{18}O plot for the soil moisture range after the transition zone for each soil type. The reduction line was placed through the average SP value of gas samples derived from < 60% water-filled pore space range for each soil. The point of intersection between the endmember mixing line and the reduction line gave the estimated initial isotope values (SP*, ^{18}O) of produced N_2O before reduction to N_2. In the soil moisture range after the transition from nitrification to

35   denitrification, if the SP* value was higher than the measured SP value of the gas sample, the measured SP value was used since N_2O reduction was assumed to be negligible. The F_N and F_D were then calculated from SP values (or SP*)

and the SP values of the nitrification and denitrification endmembers. This calculation was done for each soil type separately.

2.5 Statistical analysis

Correlation and linear regression analyses were conducted in CoStat (CoStat 6.451, CoHort.com) to determine associations between soil moisture and SP.

3. Results and Discussion

3.1 Nitrous oxide production

Nitrous oxide production during the 24-h incubation varied dramatically among the three soils, with peak N_2O production occurring at soil water contents equivalent to 70–80% WFPS (Fig. 2). Peak N_2O production was 100-fold greater from the Sutherland soil (100 ng N_2O-N g^{-1} 24-h^{-1}) compared to the Bradwell soil (1 ng N_2O-N g^{-1} 24-h^{-1}), and about 4-fold greater than that from the Asquith soil (24 ng N_2O-N g^{-1} 24-h^{-1}) (Fig. 2). This differentiation follows the same trend as soil inorganic N availability and soil organic matter, which decreased in the order: Sutherland > Asquith > Bradwell (Table 1).
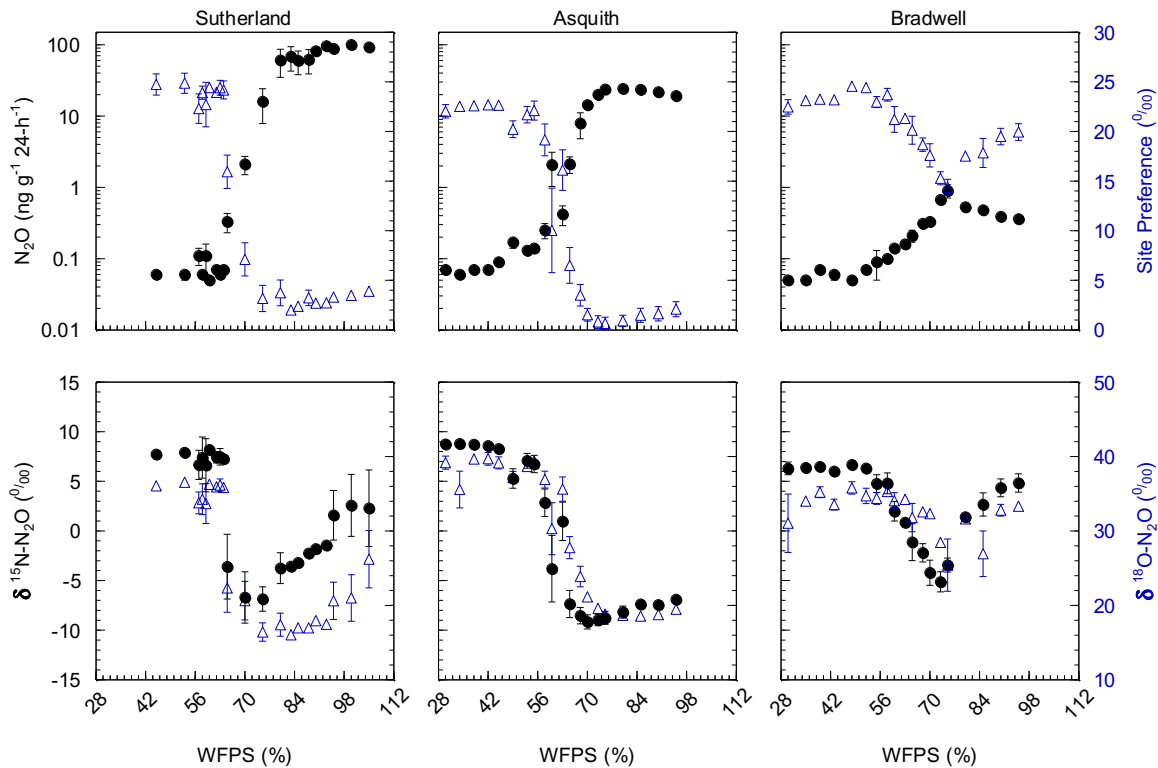
Figure 2 Top panels: N_2O production as influenced by soil water filled pore space (WFPS), (black ink, left axis); corresponding $^{15}N_2O$ isotopomer site preference (SP), (blue ink, right axis). Bottom panels: δ bulk ^{15}N (black ink, left axis) and δ ^{18}O (blue ink, right axis) of emitted N_2O as influenced by soil water filled pore space (WFPS). Note: N_2O emissions were plotted on a $\log_{10}$ scale to accommodate the large range in emissions from the different soils. Data points represent means (n = 4) and bars represent the standard errors.

Regardless of the amount of N$_2$O evolved, there were similarities in how soil moisture influenced relative N$_2$O production. For all soil types, relatively low N$_2$O fluxes were associated with drier soil treatments; N$_2$O fluxes were incrementally magnified as soil moisture levels increased from about 55 to 80% WFPS (Fig. 2, top panels). At soil moisture levels exceeding ~80% WFPS, fluxes either remained relatively high, as was the case for the Sutherland soil, or decreased slightly, as was observed for the Asquith and Bradwell soils.

3.2 Nitrous oxide ^{15}N site preference, δ ^{15}N and δ ^{18}O

Not only total N$_2$O concentration, but the ^{15}N SP, δ^{15}N and δ^{18}O of N$_2$O changed with soil moisture level, and in parallel with each other (Fig. 2, bottom panels). We identified three moisture ranges—differing slightly for each soil (Table 2)—that regulated N$_2$O production pathways based on distinct SP, δ^{15}N and δ^{18}O values (Fig. 2).

For each soil, the δ^{15}N and δ^{18}O values decreased in the same soil moisture region in which the SP values decreased (Fig. 2, bottom panels). Based on the patterns for N$_2$O fluxes, SP, δ^{15}N and δ^{18}O values as related to soil moisture (Fig. 2; Table 2), our results visually indicate there was a transition between nitrification-derived and denitrification-derived N$_2$O production at between 64 and 83; 58 and 75; 63 and 75% WFPS for the Sutherland, Asquith, and Bradwell soils, respectively.

Prior to the transition in N$_2$O production pathway, when the soil was relatively dry, the SP values averaged 23.7, 23.3, and 21.7‰ from the Sutherland, Asquith, and Bradwell soils, respectively. These values are in line with expected SP values attributed to nitrification (Denk et al., 2017; Ostrom et al., 2010; Sutka et al., 2006; Toyoda et al., 2005). Furthermore, the observed consistency among soil types – and the negligible (near 0) slopes between WFPS and ^{15}N SP – suggests that average SPs during nitrification are relatively insensitive to the rate of production or associated N$_2$O accumulation. It is known that isotopic fractionation governed by kinetic isotope effects occurs during the reaction sequence NH$_4^+$ → NH$_2$OH → NOH → NO → N$_2$O and NH$_4^+$ → NO$_2$ → NO → N$_2$O; however, oxidation of NOH does not involve a primary kinetic isotope effect and thus should not markedly affect SP (Popp et al., 2002).

During the transition from nitrification to denitrification, SP declined rapidly in all soils (Fig. 2, Table 2). The lowest SP values were 2.0, 0.7, and 14.4‰ for the Sutherland, Asquith, and Bradwell soils, respectively. In general, sharp slopes characterized the decline in SP values with increasing soil moisture during the transition; but the Sutherland and Asquith soils had steeper slopes than the Bradwell soil (Table 2). This difference was likely related to differences in soil inorganic or mineralizable N availability (Table 1) and possibly to differences in the rates of denitrification.

After the transition to denitrification, the SP values increased slightly as soil moisture increased (Table 2)—but more so for the Bradwell soil than the Sutherland and Asquith soils. This finding supports the sensitivity of SP values to the degree of stepwise completion of denitrification (N$_2$O reduction to N$_2$). We hypothesize that the ratio of N$_2$O produced to N$_2$O reduced was lowest for the Bradwell soil. Contrary to the large accrual of N$_2$O from the Sutherland and Asquith soils, the low concentration of N$_2$O produced from the Bradwell soil likely favoured complete reduction (i.e., tighter 'holes-in-the-pipe')—causing the Bradwell soil SP values to be the most sensitive to reduction of N$_2$O after the transition to denitrification (Fig. 2, Table 2). Correspondingly, using the mapping model approach to calculate the fraction of denitrified-N$_2$O reduced to N$_2$ (Lewicka-Szczebak et al., 2017) we estimated much larger fractions of N$_2$O

were reduced to N_2 at 95% WFPS in the Bradwell soil (0.47) compared to the Sutherland or Asquith soils (0.13 to 0.14) . The greater amounts of N_2O produced by the nutrient rich Sutherland and Asquith soils may have overwhelmed any reduction effect on the SP of N_2O. Our findings attribute 'N₂O leaky' soils to excess inorganic N or mineralization potential.

5   **3.3 The 'hole-in-the-pipe' influences site preference**

As alluded to above, the Bradwell results were most dissimilar to the other soils. It is intriguing that the SP values for the Bradwell soil N_2O never dropped below 14.4‰. While it is clear from the pattern of N_2O fluxes, SP, $\delta^{15}N$ and $\delta^{18}O$ values (Fig. 2) that N_2O production transitioned to denitrification as the soil water content was increased (Table 2), it is curious that the SP values were not lower (i.e., closer to 0‰) as earlier work demonstrated for denitrification

10   (Denk et al., 2017; Ostrom et al., 2010; Sutka et al., 2006; Toyoda et al., 2005; Winther et al., 2018). Reasons for this discrepancy are as yet unclear, but we are not alone in finding SP values above 0‰ that are attributed to denitrification (Winther et al., 2018). Differences might be related to differences in microbial community structure and activity, as suggested by Decock and Six (2013a). Also, it is very likely that multiple processes underlying N_2O production and consumption acted simultaneously to cause a higher than expected SP value (Decock and Six, 2013a). Otherwise, N_2O

15   reduction to N_2 might have played a larger than anticipated role for the Bradwell soil. Indeed, SP values within the expected range for bacterial denitrification are known to be sensitive to the reduction of N_2O to N_2 (Deppe et al., 2017; Jinuntuya-Nortman et al., 2008; Lewicka-Szczebak et al., 2014; Ostrom et al., 2007; Well and Flessa, 2009). Despite similarities among soils in the robust patterns of how SP values are influenced by soil moisture (Fig. 2; Table 2), SP exhibited a significant ($P < 0.0001$) soil × moisture region interaction. This finding agrees with earlier suggestions

20   that, at finer scales, the $^{15}N_2O$ isotopic signatures and SP values are likely regulated by the active soil microbial community, process rates, soil heterogeneity (Decock and Six, 2013a; Lewicka-Szczebak et al., 2014). Denitrification results in cleavage of the covalent bond between the central N and O in N_2O, and based on kinetic isotope fractionation results in an increase in the ^{15}N content of the α position of the residual N_2O, thereby increasing the SP (Popp et al., 2002; Ostrom et al., 2007). Thus, the increase in SP in response to N_2O reduction results in a small (but important)

25   shift away from the SP values associated with the origins of denitrification (~ 0‰) towards those of nitrification, i.e., 33‰ (Sutka et al., 2006). Previously, the fractionation of SP due to N_2O reduction was constrained to a variation of -2‰ to -8‰ (Jinuntuya-Nortman et al., 2008; Lewicka-Szczebak et al., 2014; Well and Flessa, 2009). Ostrom et al. (2007) showed that the rate of reduction must be substantially greater than 10% that of production to impact the SP estimates of N_2O from denitrification by more than a few percent. Because it is likely that N_2O consumption was

30   greater than production for the Bradwell soil when soil moisture exceeded 75% WFPS, our results indicate that the 'size of the hole-in-the-pipe' may influence denitrification SP to a greater extent than previously documented.

For N_2O source identification, we adopted an isotopomer mixing approach (Deppe et al., 2017; Lewicka-Szczebak et al., 2017; Zou et al., 2014) and constructed isotopomer maps (i.e., plots of SP *vs.* $\delta^{18}O$). This approach allowed us to estimate the impact of N_2O reduction to N_2 on SP. Reduction slopes for our three soils averaged 0.28, which is similar

35   to the literature-derived average of 0.35 or. 0.33 used by Deppe et al. (2017) and Lewicka-Szczebak et al. (2017), respectively, though they varied over a wide range; i.e., from 0.16 to 0.52 (Fig. 3). A high reduction slope, such as

observed for the Bradwell soil, might be associated with the magnitude of N_2O production relative to potential nitrous oxide reductase activity, or conditions that favour more complete stepwise reduction of N_2O to N_2. Whereas the reduction effect on SP might be stronger than previously thought, it may only be observable when conditions are favourable, as evidenced for the Bradwell soil. We echo earlier proposals made by Ostrom et al. (2007), and suggest that the current knowledge and understanding of $^{15}N_2O$ isotopomers may have inherent biases due to methodological focus on high flux scenarios – where the rates of N_2O reduction are minor and likely not of sufficient magnitude to alter isotopomer and SP data. Relatively few studies have focused on lower flux scenarios when the rates of N_2O reduction relative to production may exert more of an influence on SP. Our findings support the hypothesis that N_2O reduction is a minor process influencing SP during conditions of high soil N_2O flux, but may be more important for conditions with low N_2O flux (Ostrom et al., 2007).
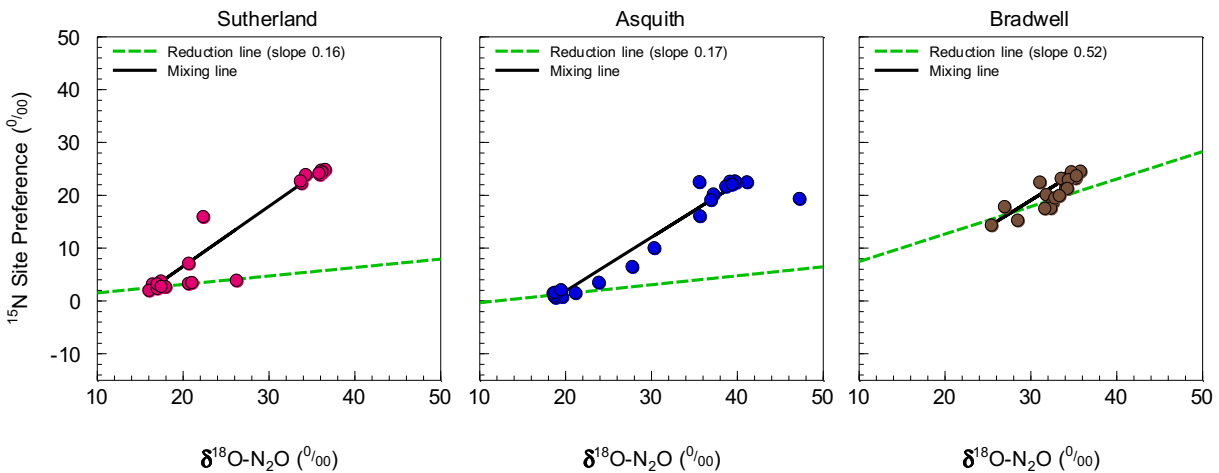
Figure 3 Isotopomer map to determine the source partitioning of N_2O derived from nitrification versus denitrification using mean (n = 4) ^{15}N site preference (SP) and $\delta^{18}O$ of N_2O. The linear mixed model approach was based on Deppe et al. 2017 and Lewicka-Szczebak et al. (2017), but with mixing line end-members and reduction line slopes derived from our data..

Due to the wide range of reduction slopes observed in our study—and the differences for how SP is influenced in conditions with high flux *vs* low flux—we argue that using a single average reduction slope is insufficient to best predict N_2O reduction. This finding echoes earlier work which suggested that during soil conditions when processes of N_2O production and reduction occur simultaneously, the reduction line approach may be limited (Decock and Six, 2013b). It is recommended that further research better quantify the conditions that promote N_2O reduction for improved N_2O source predictions. This could be particularly important for assessing microbial source pathways of N_2O production and consumption across seasonal and spatial scales, because sustained periods of low flux are not uncommon.

3.4 Source pathway partitioning and modelling

Using the pooled data from the isotopomer maps to predict source partitions, linear models were developed that fit the transitions for nitrification-derived N_2O ($R^2 = 0.65$, $p < 0.001$) and denitrification-derived N_2O ($R^2 = 0.65$, $p < 0.001$)

(Fig. 4) with coefficients of variation and root-mean-square errors of 0.10 and 0.20, respectively. The models predict that over a soil moisture range of 53 to 78% WFPS, the source partitioning rapidly changed from nitrification- to denitrification-dominated N_2O production. At soil moisture levels < 53% WFPS, N_2O was predominately attributed to nitrification ($F_N = 1$) but thereafter decreased rapidly, according to Eq. (6):

$$F_N = 3.19 - 0.041x \tag{6}$$

until a WFPS of 78%. This result was mirrored by the increase in N_2O attributed to denitrification at a WFPS of 53% according to Eq. (7):

$$F_D = -2.19 + 0.041x \tag{7}$$

until $F_D = 1$ at 78% and higher WFPS. These relationships exemplify the sensitivity of N_2O production pathways to soil moisture changes. For instance, during the transition, a change in soil moisture as little as 10% (i.e., from 55 to 65% WFPS) is predicted to lower nitrification-derived N_2O production by 56% but increase denitrification-derived N_2O by >7-fold (Fig. 4). Consequently, the linear models presented here may help other researchers estimate N_2O source partitioning when soil moisture falls within the transition from nitrification to denitrification.
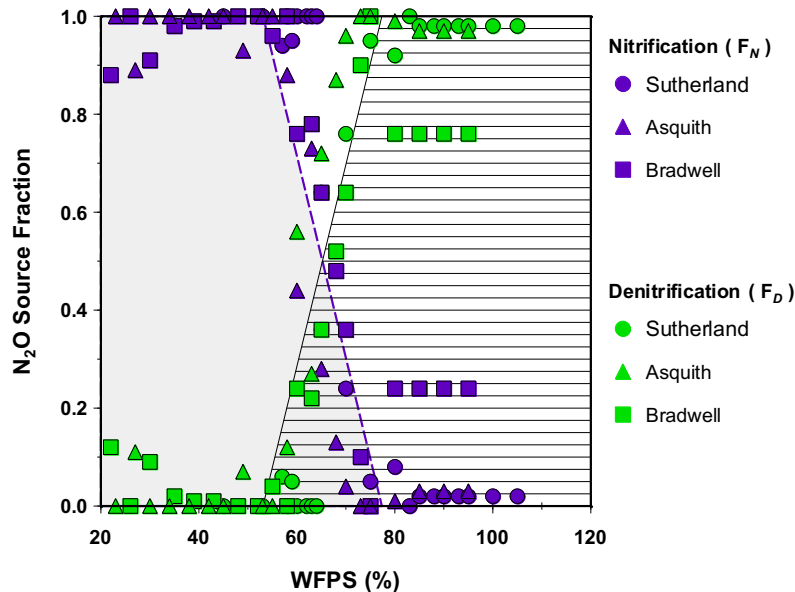
Figure 4 Fraction of emitted N_2O that was attributed to nitrification (F_N; shaded grey area) or denitrification (F_D; lined area) based on the isotopomer mixing model (data points). Note: the dashed purple line denotes the predicted F_N (Eq. 6); the solid black line denotes the predicted F_D (Eq. 7).

As a check, the soil-specific approach presented here was compared to the independent endmember/slope approach commonly used by other researchers (Deppe et al., 2017; Lewicka-Szczebak et al., 2017). Isotopomer maps were calculated using independent literature-derived values (see Fig. S1) with the endmembers set at -2.4 to 34.4 for SP_D to SP_N, and 11.1 to 43.0 for $\delta^{18}O_D$ to $\delta^{18}O_N$; and a reduction slope of 0.33 (Lewicka-Szczebak et al., 2017). Using the

literature-derived endmembers overestimated the contribution of denitrification-derived N_2O under very dry soil conditions (i.e., 20 to 40% WFPS)—indicating that up to 40% of N_2O produced under these conditions was a result of denitrification (Fig. S1)—a contradiction to common knowledge (Butterbach-Bahl et al., 2013; Davidson et al. 1991). In our case, N_2O source partitioning using soil-specific endmembers provided an advantage over using independent endmembers because the endmembers for the Bradwell soil were different from the literature-derived values; likely due to real soil biological processes such as microbial communities, the low rate of production, or soil heterogeneity (Decock and Six, 2013a; Lewicka-Szczebak et al., 2014). Nonetheless, we recommend that future research aims to develop more advanced models that take into account variability or more nuanced isotope effects.

Clearly, soil moisture change during the transition is a key regulator of which pathway dominantly produces N_2O— be it nitrification or denitrification, or a mixture of both. Our results largely support the foundational studies that established the relationship between soil moisture and N_2O emissions (Davidson, 1991; Linn and Doran, 1984); however, we provide a method that moves beyond just inferring N_2O source pathways towards quantifying the pathway contributions over a range of soil moisture—and does so without having to add a ^{15}N label.

4 Conclusions

Determining the production pathways of soil-derived N_2O is a worthwhile goal as there is potential to manage soils in ways that lead to reduced nitrification or denitrification during periods of risk for N_2O loss—thereby mitigating emissions of a potent greenhouse gas. We show that isotopomer data have the potential to provide progress towards this goal. Measuring $^{15}N_2O$ isotopomers enabled a more precise evaluation of the relationship between soil moisture and N_2O production and we present a source fraction model for key soil moisture ranges. In general, our results support earlier assumptions about the relationships between moisture and N_2O production pathways but can help move beyond inferring towards quantifying relative source pathways. Clearly, soil moisture level during 'the transition zone' is a key regulator of which pathway predominates—be it nitrification, denitrification, or a mixture of both. Hence, the models presented herein should be useful for other researchers to estimate contributions of nitrification versus denitrification when soil WFPS ranges from 53-78%.

One known caveat when using the isotopomer method for source pathway quantification is the isotope effect of N_2O reduction. Previous researchers have attempted to address this limitation by using an average reduction slope and linear mixed model approach, but due to the wide range of reduction slopes observed in our study—and the differences for how denitrification SP is influenced in conditions with high N_2O flux *vs* low flux—we argue that using a single average reduction slope is insufficient to best predict N_2O reduction. It is recommended that further research better quantify the conditions which influence N_2O reduction and its sensitivity on denitrification SP values for improved N_2O source predictions. The creation of larger isotope databases would contribute to the development of more advanced models that take into account variability or more nuanced isotope effects.

5 Author Contributions

KAC and REF designed the experiment and TP carried it out. KAC prepared the manuscript with contributions from REF and TP.

6 Competing Interests

The authors declare that they have no conflict of interest.

5 **7 Acknowledgements**

Financial support was provided by the University of Saskatchewan College of Agriculture and Bioresources via a Martin Agricultural Trust Fund award to KAC and REF and by the Natural Sciences and Engineering Research Council of Canada via a Discovery Grant award to KAC. The authors are grateful to Frank Krijnen and Darin Richman for technical help in the lab.

10 **8 References**

Balaine, N., Clough, T. J., Beare, M. H., Thomas, S. M., Meenken, E. D. and Ross, J. G.: Changes in Relative Gas Diffusivity Explain Soil Nitrous Oxide Flux Dynamics, Soil Sci. Soc. Am. J., 77(5), 1496–1505, doi:DOI 10.2136/sssaj2013.04.0141, 2013.

Banerjee, S., Helgason, B., Wang, L., Winsley, T., Ferrari, B. C. and Siciliano, S. D.: Legacy effects of soil moisture
15 on microbial community structure and N_2O emissions, Soil Biol. Biochem., 95, 40–50, doi:10.1016/J.SOILBIO.2015.12.004, 2016.

Barnard, R., Leadley, P. W. and Hungate, B. A.: Global change, nitrification, and denitrification: A review, Global Biogeochem. Cycles, 19(1), doi:10.1029/2004GB002282, 2005.

Bateman, E. and Baggs, E.: Contributions of nitrification and denitrification to N_2O emissions from soils at different
20 water-filled pore space, Biol Fertil Soils, 41, 379–388, doi:10.1007/s00374-005-0858-3, 2005.

Butterbach-Bahl, K., Baggs, E. M., Dannenmann, M., Kiese, R. and Zechmeister-Boltenstern, S.: Nitrous oxide emissions from soils: how well do we understand the processes and their controls?, Philos. Trans. R. Soc. Lond. B. Biol. Sci., 368(1621), 20130122, doi:10.1098/rstb.2013.0122, 2013.

Chapuis-Lardy, L., Wrage, N., Metay, A., Chotte, J.-L. and Bernoux, M.: Soils, a sink for N_2O? A review, Glob.
25 Chang. Biol., 13(1), 1–17, doi:10.1111/j.1365-2486.2006.01280.x, 2007.

Clough, T. J., Sherlock, R. R. and Rolston, D. E.: A Review of the Movement and Fate of N_2O in the Subsoil, Nutr. Cycl. Agroecosystems, 72(1), 3–11, doi:10.1007/s10705-004-7349-z, 2005.

Davidson, E. A.: Fluxes of nitrous oxide and nitric oxide from terrestrial ecosystems. Pp. 219–235 in Rogers J.E., Whitman, W.B. eds . Microbial Production and Consumption of Greenhouse Gases: Methane, Nitrogen Oxides and
30 Halomethanes, Am. Soc. Microbiol. Washington, DC., in Microbial Production and Consumption of Greenhouse Gases: Methane, Nitrogen Oxides and Halomethanes, edited by J. E. Rogers and W. B. Whitman, pp. 219–235, Am. Soc. Microbiol., Washington, DC., 1991.

Decock, C. and Six, J.: How reliable is the intramolecular distribution of ^{15}N in N_2O to source partition N_2O emitted from soil?, Soil Biol. Biochem., 65(2), 114–127, doi:10.1016/j.soilbio.2013.05.012, 2013a.

Decock, C. and Six, J.: On the potential of $\delta^{18}O$ and $\delta^{15}N$ to assess N_2O reduction to N_2 in soil, Eur. J. Soil Sci., 64(5), 610–620, doi:10.1111/ejss.12068, 2013b.

Denk, T. R. A., Mohn, J., Decock, C., Lewicka-Szczebak, D., Harris, E., Butterbach-Bahl, K., Kiese, R. and Wolf, B.: The nitrogen cycle: A review of isotope effects and isotope modeling approaches, Soil Biol. Biochem., 105, 121–137, doi:10.1016/J.SOILBIO.2016.11.015, 2017.

Deppe, M., Well, R., Giesemann, A., Spott, O. and Flessa, H.: Soil N_2O fluxes and related processes in laboratory incubations simulating ammonium fertilizer depots, Soil Biol. Biochem., 104, 68–80, doi:10.1016/j.soilbio.2016.10.005, 2017.

Environment Canada: Canadian national Inventory Report: Part 3 Greenhouse gas sources and sinks in Canada., 2015.

Groffman, P.M., Altabet, M.A., Bohlke, J.K., Butterbach-Bahl, K., David, M.B., Firestone, M.K., Giblin, A.E., Kana, T.M., Neilsen, L.P., and Voytek, M.A.: Methods for measuring denitrification: Diverse approaches to a difficult problem. Ecol. Appl. 16,2091–2122, 2006.

McNaught, A.D. and Wilkinson, A.: IUPAC Compendium of Chemical Terminology – The Gold Book, 2nd Edition, Blackwell Science Ltd., Oxford, United Kingdom, 1997.

Jinuntuya-Nortman, M., Sutka, R. L., Ostrom, P. H., Gandhi, H. and Ostrom, N. E.: Isotopologue fractionation during microbial reduction of N_2O within soil mesocosms as a function of water-filled pore space, Soil Biol. Biochem., 40(9), 2273–2280, doi:10.1016/J.SOILBIO.2008.05.016, 2008.

Lewicka-Szczebak, D., Well, R., Köster, J. R., Fuß, R., Senbayram, M., Dittert, K. and Flessa, H.: Experimental determinations of isotopic fractionation factors associated with N_2O production and reduction during denitrification in soils, Geochim. Cosmochim. Acta, 134, 55–73, doi:10.1016/J.GCA.2014.03.010, 2014.

Lewicka-Szczebak, D., Augustin, J., Giesemann, A. and Well, R.: Quantifying N_2O reduction to N_2 based on N_2O isotopocules-validation with independent methods (helium incubation and ^{15}N gas flux method), Biogeosciences, 14(3), 711–732, doi:10.5194/bg-14-711-2017, 2017.

Linn, D. M. and Doran, J. W.: Effect of water-filled pore space on carbon dioxide and nitrous oxide production in tilled and nontilled soils, Soil Sci. Soc. Am. J., 48(6), 1267–1272, doi:10.2136/sssaj1984.03615995004800060013x, 1984.

Maynard, D., Kalra, Y. and Crumbaugh, J.: Nitrate and exchangeable ammonium nitrogen, in Soil Sampling and Methods of Analysis, edited by M. R. Carter and E. G. Gregorich, pp. 71–80, CRC Press, Boca Raton, Florida. [online] Available from: https://books.google.ca/books?hl=en&lr=&id=54lYLsV49zIC&oi=fnd&pg=PA25&dq=Nitrate+and+exchangeable+ ammonium+nitrogen&ots=K2iO0IE4wU&sig=OzBHEHi8c7pEvx7dvHR7Sk3F3bM (Accessed 8 December 2015), 2007.

Mohn, J., Wolf, B., Toyoda, S., Lin, C.-T., Liang, M.-C., Brüggemann, N., Wissel, H., Steiker, A. E., Dyckmans, J., Szwec, L., Ostrom, N. E., Casciotti, K. L., Forbes, M., Giesemann, A., Well, R., Doucett, R. R., Yarnes, C. T., Ridley, A. R., Kaiser, J. and Yoshida, N.: Interlaboratory assessment of nitrous oxide isotopomer analysis by isotope ratio mass spectrometry and laser spectroscopy: current status and perspectives, Rapid Commun. Mass Spectrom., 28(18), 1995–2007, doi:10.1002/rcm.6982, 2014.

Ostrom, N. E. and Ostrom, P. H.: The Isotopomers of Nitrous Oxide: Analytical Considerations and Application to Resolution of Microbial Production Pathways, in Handbook of Environmental Isotope Geochemistry, pp. 453–476, Springer Berlin Heidelberg, Berlin, Heidelberg., 2012.

5   Ostrom, N. E., Pitt, A., Sutka, R., Ostrom, P. H., Grandy, A. S., Huizinga, K. M. and Robertson, G. P.: Isotopologue effects during N_2O reduction in soils and in pure cultures of denitrifiers, J. Geophys. Res., 112(G2), G02005, doi:10.1029/2006JG000287, 2007.

Ostrom, N. E., Sutka, R., Ostrom, P. H., Grandy, A. S., Huizinga, K. M., Gandhi, H., von Fischer, J. C. and Robertson, G. P.: Isotopologue data reveal bacterial denitrification as the primary source of N_2O during a high flux event following cultivation of a native temperate grassland, Soil Biol. Biochem., 42(3), 499–506,

10 doi:10.1016/J.SOILBIO.2009.12.003, 2010.

Perez, T., Trumbore, S. E., Tyler, S. C., Matson, P. a., Ortiz-Monasterio, I., Rahn, T. and Griffith, D. W. T.: Identifying the agricultural imprint on the global N_2O budget using stable isotopes, J. Geophys. Res., 106(D9), 9869–9878, doi:10.1029/2000JD900809, 2001.

Popp, B. N., Westley, M. B., Toyoda, S., Miwa, T., Dore, J. E., Yoshida, N., Rust, T. M., Sansone, F. J., Russ, M.

15 E., Ostrom, N. E. and Ostrom, P. H.: Nitrogen and oxygen isotopomeric constraints on the origins and sea-to-air flux of N2O in the oligotrophic subtropical North Pacific gyre, Global Biogeochem. Cycles, 16(4), 12-1-12–10, doi:10.1029/2001GB001806, 2002.

Reynolds, W. D. and Topp, G. C.: Soil Water Desorption and Imbibition : Long Column, in Soil Sampling and Methods of Analysis, edited by M. R. Carter and E. G. Gregorich, pp. 999–1006., 2007.

20 Stevens, R. J. and Laughlin, R. J.: Measuring the contributions of nitrification and denitrification to the flux of nitrous oxide from soil, , 29(2), 139–151, 1997.

Sutka, R. L., Ostrom, N. E., Ostrom, P. H., Breznak, J. A., Gandhi, H., Pitt, A. J. and Li, F.: Distinguishing nitrous oxide production from nitrification and denitrification on the basis of isotopomer abundances., Appl. Environ. Microbiol., 72(1), 638–44, doi:10.1128/AEM.72.1.638-644.2006, 2006.

25 Toyoda, S. and Yoshida, N.: Determination of nitrogen isotopomers of nitrous oxide on a modified isotope ratio mass spectrometer, Anal. Chem., 71(20), 4711–4718, doi:10.1021/ac9904563, 1999.

Toyoda, S., Mutobe, H., Yamagishi, H., Yoshida, N. and Tanji, Y.: Fractionation of N_2O isotopomers during production by denitrifier, Soil Biol. Biochem., 37(8), 1535–1545, doi:10.1016/j.soilbio.2005.01.009, 2005.

Van Groenigen, J. W., Huygens, D., Boeckx, P., Kuyper, T. W., Lubbers, I. M., Rütting, T. and Groffman, P. M.:

30 The soil N cycle: new insights and key challenges, Soil, 1, 235–256, doi:10.5194/soil-1-235-2015, 2015.

Wagner-Riddle, C., Congreves, K. A., Abalos, D., Berg, A. A., Brown, S. E., Ambadan, J. T., Gao, X. and Tenuta, M.: Globally important nitrous oxide emissions from croplands induced by freeze-thaw cycles, Nat. Geosci., 10(4), doi:10.1038/ngeo2907, 2017.

Well, R. and Flessa, H.: Isotopologue signatures of N2O produced by denitrification in soils, J. Geophys. Res.

35 Biogeosciences, 114(G2), n/a-n/a, doi:10.1029/2008JG000804, 2009.

Winther, M., Balslev-Harder, D., Christensen, S., Priemé, A., Elberling, B., Crosson, E. and Blunier, T.: Continuous measurements of nitrous oxide isotopomers during incubation experiments, Biogeosciences, 15, 767–780, doi:10.5194/bg-15-767-2018, 2018.

Yamulki, S., Toyoda, S., Yoshida, N., Veldkamp, E., Grant, B. and Bol, R.: Diurnal fluxes and the isotopomer ratios of N_2O in a temperate grassland following urine amendment, Rapid Commun. Mass Spectrom., 15(15), 1263–1269, doi:10.1002/rcm.352, 2001.

Yoshida, N. and Toyoda, S.: Constraining the atmospheric N_2O budget from intramolecular site preference in N_2O isotopomers, Nature, 405(6784), 330–334, doi:10.1038/35012558, 2000.

Zou, Y., Hirono, Y., Yanai, Y., Hattori, S., Toyoda, S. and Yoshida, N.: Isotopomer analysis of nitrous oxide accumulated in soil cultivated with tea (Camellia sinensis) in Shizuoka, central Japan, Soil Biol. Biochem., 77, 276–291, doi:10.1016/j.soilbio.2014.06.016, 2014.

Table 1 Soil physical and chemical characteristics.

	Sutherland	Asquith	Bradwell
Previous cropping history	Vegetable crops	Fodder crops	Field crops
Texture class	Silty clay loam	Sandy loam	Loam
Organic matter (%)	5.9	3.9	2.7
Equilibrium soil water (θg)	0.46	0.40	0.33
pH	7.6	7.5	7.9
CEC cmol$_c$ kg^{-1}	34.8	18.6	16.9
Total N (%)	0.42	0.21	0.16
Total ^{15}N (atom %)	0.371	0.370	0.368
Nitrate (μg g^{-1})	194	35	10
Ammonium (μg g^{-1})	3.8	1.7	5.2
Bray-Phosphorus (ppm)	542	190	23
Potassium (ppm)	1415	544	329
Sulfur (ppm)	49	28	13
Magnesium (ppm)	925	448	432
Calcium (ppm)	4650	2670	2490

Table 2. Linear regressions between ^{15}N site preference and soil water-filled pore space (%) during three soil moisture regions for each soil type: i) before the transition from nitrification, ii) during the transition from nitrification to denitrification, and iii) after the transition to denitrification.

Soil type	WFPS (%)	Slope	Intercept	Pearson r	*p*-value
Before transition					
Sutherland	< 64	-0.049	26.69	-0.30	0.4660 [ns]
Asquith	< 58	-0.004	22.04	-0.04	0.8973 [ns]
Bradwell	< 63	0.010	22.69	0.14	0.6781 [ns]
During transition					
Sutherland	64 – 83	-0.99	81.62	0.88	0.0214*
Asquith	58 – 73	-1.19	85.75	-0.89	0.0067**
Bradwell	63 – 75	-0.59	58.29	-0.99	0.0004*
After transition					
Sutherland	> 83	0.065	-3.01	0.86	0.0126*
Asquith	> 73	0.072	-4.77	0.99	0.0064**
Bradwell	> 75	0.262	-4.47	0.94	0.0154*